

UC Berkeley

UC Berkeley Previously Published Works

Title

Optimal policies for greenhouse gas emission minimization under multiple agency budget constraints in pavement management

Permalink

<https://escholarship.org/uc/item/19h88309>

Authors

Lee, Jinwoo
Madanat, Samer

Publication Date

2017-08-01

DOI

10.1016/j.trd.2017.06.009

Peer reviewed

Optimal policies for Greenhouse gas emission minimization under multiple
agency budget constraints in pavement management

Jinwoo Lee*

Division of Engineering

New York University Abu Dhabi

Abu Dhabi, 129188, United Arab Emirates

Phone: +971 2-628-4557

Email: jinwoo.lee@nyu.edu

Samer Madanat

Division of Engineering

New York University Abu Dhabi

Abu Dhabi, 129188, United Arab Emirates

Phone: +971 2-628-4881

Email: samer.madanat@nyu.edu

*: Corresponding Author

ABSTRACT

Greenhouse gas emissions reduction has garnered special importance in recent times in the transportation sector, including pavement design and management. In this study, we incorporate this environmental objective in pavement management. We present an optimization problem to minimize GHG emissions under multiple budget constraints by determining joint management strategies for a range of heterogeneous interventions, including maintenance, rehabilitation and reconstruction. We propose a computationally efficient bottom-up solution algorithm, which is built on Lagrangian Relaxation and Dynamic Programming. Finally, we apply our findings to a real-world highway network in California, where the results show a potential GHG emissions reduction of 20% through an increased combined budget of 35% on the Pareto frontier.

Keywords: Pavement Management Systems; Greenhouse Gas Emissions; Budget Constraints

1. Introduction

We present a decision support tool in Pavement Management Systems (PMSs) to reduce Greenhouse gas (GHG) emissions under budget constraints. GHG emissions caused by societal activities are known to be forcing global climate changes (Foster et al., 2007), with the transportation sector being one of the most GHG emission contributors in the USA second to the electricity generation sector. Highway transportation produces over 80 percent of GHG emissions of the transportation sector, including passenger cars (42.3 percent), light-duty trucks (17.1 percent) and medium- and heavy- duty trucks (23.6 percent) (EPA, 2017), and the highway user emissions increase with pavement roughness level (Watanatada, 1986; Zaabar and Chatti, 2010). Therefore, reducing roughness-related pavement emissions may make a significant dent in the total transportation sector GHG emissions (Santero et al., 2011).

In PMSs, transportation agencies have multiple options of interventions with different costs and impacts on pavement condition. For instance, the California Department of Transportation (Caltrans) considers five management options targeted at different pavement condition, including: preventive maintenance, corrective maintenance, capital preventive maintenance, major rehabilitation, and reconstruction (Caltrans, 2015). Several papers in the literature have considered heterogeneous management treatments as decision factors in minimizing pavement life cycle costs, for the segment-level problem (Gu et al., 2012; Rashid and Tsunokawa, 2012; Lee and Madanat, 2014 and 2015a) and the system-level problem (Chu and Chen, 2012; Lee and Madanat, 2015b). In this paper, we include three types of interventions: routine maintenance activities, rehabilitations, and reconstructions (MR&R).

Numerous studies have addressed the problem of minimizing GHG emissions in PMS through Life Cycle Assessment (LCA). Wang et al (2012) and Lidicker et al. (2013) examined management strategies to minimize GHG emissions at a pavement segment level. Gosse et al. accounted for multiple criteria including system performance as well as emissions and costs from management activities. At the pavement system level, research has focused on both minimizing GHG emissions (Wang et al., 2014) and minimizing lifecycle societal costs under a constraint of total GHG emissions (from users and agencies). Examples of the latter include Reger et al. (2014), who solved for the optimal

rehabilitation policy, and Lee et al. (2016), who solved for the optimal mix of rehabilitation and reconstruction strategies. One limitation of this line of work is that the objective function, minimizing societal costs under an emissions budget, may not be a realistic representation of a highway agency's problem.

This research builds upon the work of Reger et al. (2015), where the problem formulation is to find the pavement resurfacing strategy to minimize system-level GHG emissions under a financial budget constraint, a more realistic representation of the problem facing highway agencies. The difference with Reger et al. (2015) is that, in the present paper a range of interventions is considered rather than focusing only on resurfacing. Given the wide range of interventions considered, multiple budget constraints are used to account for multiple budget sources. Another, more technical difference is that the present research uses a more realistic history-dependent pavement deterioration model and considers the problem along both finite and infinite planning horizons. This paper is organized as follows: Section 2 presents the problem formulation. The solution methodology is proposed in Section 3. A case study is included in Section 4 and conclusions follow in Section 5.

2. Problem formulation

In this section, we formulate an average Greenhouse gas (GHG) emission minimization problem under budget constraints for a system comprised of N pavement segments along a planning horizon of length T . Sub-sections 2.1 and 2.2. present the objective function and the budget constraints of the problem respectively.

2.1 Objective

The objective function is formulated in (1), where the system-level average GHG emissions for both users and agencies are considered. The decision factor is the pavement management policy, x , which is a set of segment-level policies, x_n , for all segments included in the system, i.e. $x = \{x_1, \dots, x_n, \dots, x_N\}$. x_n is a set defined as $\{x_n(0), \dots, x_n(t), \dots, x_n(T - 1)\}$. The segment-level pavement state in period t ,

$S_n(t) \in \mathbb{S}_n$, is defined as a multi-dimensional vector that consists of various distresses and history-dependent factors. In this paper, $E[\cdot]$ represents expected value.

$$\min_{x \in \mathbb{X}} Q(S(0), x) = \min_{x_n, \forall n} \sum_{n=1}^N Q_n(S_n(0), x_n) = \min_{\substack{x_n(t) \in \mathbb{X}_n \\ \forall n, t}} \frac{1}{T} E \left[\sum_{n=1}^N \sum_{t=0}^{T-1} q_n(S_n(t), x_n(t)) \right] \quad (1)$$

, where

\mathbb{X} : a set of all possible policies;

\mathbb{X}_n : a set of all available managerial options on a segment;

$Q(S(0), x)$: undiscounted average GHG emission (metric tons (MT) CO₂ e/unit time period) for the system of pavements with an initial state $S(0) \equiv \{S_n(0), \forall n\}$, under policy x ;

$Q_n(S_n(0), x_n)$: undiscounted average GHG emission for segment n with an initial state, $S_n(0)$ under policy x_n ;

$q_n(S_n(t), x_n(t))$: GHG emissions for segment n during period t with state $S_n(t)$, under policy $x_n(t)$;

T : length of planning horizon;

N : total number of pavement segments.

2.1.1 GHG emissions

We do not use a discount rate for GHG emissions, in accordance with Sedjo and Marland (2003) who made the case that future GHG emissions should not be discounted. However, Kendall (2012) argued that it is necessary to use the time-adjusted measure to prevent distorting the actual influence of GHG emissions in the future. If we use the time correction factor to consider this effect, the GHG minimization problem with the budget constraint can be formulated as a mixed-undiscounted-and-discounted problem. The solution methodology for such a problem can be found in Lee and Madanat (2016). In this paper, we focus on the undiscounted problem that has not been addressed and solved in the literature.

In equation (1), $q_n(S_n(t), x_n(t))$ is the sum of user emissions and agency emissions caused by the activities applied on the segment $x_n(t)$ with state $S_n(t)$. The sources of user emissions are: additional fuel consumption caused by high roughness (Watanatada, 1986; Zaabar and Chatti, 2010),

which can be reduced due to a smoother surface resulting from MR&R activities; and travel time and distance delay due to roadway closures during the activities. For the option of ‘do-nothing’, agency emissions are zero. If at least one intervention is applied, agency emissions are produced along the supply chain of used materials from production to transportation to the site and determined by the nature of construction activities.

2.1.2 Pavement state and deterioration model

The elements of the pavement state vector $S_n(t)$ are surface roughness, $s_n(t)$, measured in units of International Roughness Index (IRI) (m/km), and age or the elapsed time since the last construction or reconstruction given by $h_n(t)$ (year). The transition probability, from one state, at t , to another, at $t + 1$, is dependent on exogenous factors (e.g. site-specific traffic loading and climate) and endogenous factors (such as history of past interventions). This bi-dimensional state at a time t reflects all the effects of previous states and performed interventions, because:

1. If a pavement was reconstructed at least once after its initial construction, the applied interventions and pavement states before the most recent reconstruction have no effect on the deterioration process, and thus the only period of time relevant to predict future pavement condition is time since the last reconstruction (i.e., age).

2. The underlying layers’ (base and sub-base) condition is not improved by rehabilitation and routine maintenance because these activities are performed only on the surface (wearing course) layer. Thus, age accounts for the deterioration of the underlying layers.

3. The surface layer condition is a complete representation of all maintenance and rehabilitation interventions performed on the surface layer since the last reconstruction.

Because $S_n(t)$ accounts for all the relevant history of pavement segment n at time t , it can be concluded that the evolution of the (augmented) pavement state $S_n(t)$ is Markovian.

2.2 Budget constraints

It is typical that different pavement interventions are funded by different budget sources. For example, construction and reconstruction projects are funded by a capital budget, but other managerial interventions including routine maintenance and rehabilitation are financed by a maintenance budget. The general representation of budget constraints is represented in (2a), where we assume flexible budget allocation between different periods.

$$A_j(S(0), x) = \sum_{n=1}^N A_{n,j}(S_n(0), x_n) = \frac{1}{T} E \left[\sum_{n=1}^N \sum_{t=0}^{T-1} a_{n,j}(S_n(t), x_n(t)) \right] \leq B_j, \forall j = 1, \dots, J \quad (2a)$$

, where

$A_j(S(0), x)$: average agency costs (\$/unit time period) for a system of pavement segments with an initial state $S(0)$ under policy x constrained by budget j , $j \in \{1, \dots, J\}$;

J : number of constraints, i.e. number of budget sources;

$a_{n,j}(S_n(t), x_n(t))$: agency costs in period t funded by budget j ;

B_j : budget j , $j \in \{1, \dots, J\}$.

If there are multiple budget expenditure periods in the planning horizon, indexed by $w = 1, \dots, W$, the budget constraints are represented as:

$$A_{j,w}(S(T_0 + \dots T_{w-1}), x) = \frac{1}{T_w} E \left[\sum_{n=1}^N \sum_{t=T_0+\dots T_{w-1}}^{T_0+\dots T_w-1} a_{n,j}(S_n(t), x_n(t)) \right] \leq B_j, \quad (2b)$$

$$\forall j = 1, \dots, J, \forall w = 1, \dots, W,$$

, where

$A_{j,w}(S(T_0 + \dots T_{w-1}), x)$: average agency costs (\$/unit time period) for a system of pavement segments constrained by budget j during budget expenditure period w ;

T_w : duration of the w^{th} budget expenditure period, $T_0 = 0$;

W : number of budget expenditure periods in T years, $T_0 + \dots T_W = T$.

3. Solution methodology

The constrained optimization problem is solved by the Lagrangian Relaxation method (Bellman, 1956).

In Section 3.1, we propose a solution methodology for the problem defined by (1) and (2a). Section 3.2

present the solution methodology for the problem with multiple budget expenditure periods, $W > 1$, defined by (1) and (2b).

3.1 Flexible budget allocation problem

The optimal Lagrangian function, $\mathcal{L}^*(S(0))$, the lower bound of the original problem, with non-negative Lagrangian multiplier $\Lambda = \{\Lambda_1, \dots, \Lambda_j, \dots, \Lambda_J\}$ is given in equation (3). Note that the unit of each Lagrangian multiplier is metric tons of CO_2 per dollar, so all terms in (3) have the same dimensions. In (3), the decision variables are $\{x; \Lambda\}$, and the solution method has two steps: (a) to find the optimal x for given Lagrangian multiplier, denoted by $x_{|\Lambda}$; and (b) to find the optimal Lagrangian multiplier, Λ .

$$\mathcal{L}^*(S(0)) = \sup_{\Lambda} \min_x Q(S(0), x) + \sum_{j=1}^J \Lambda_j \cdot [A_j(S(0), x) - B_j] \quad (3)$$

To separate the system-level problem (3) into N segment-level problems, we assume that:

Assumption 1. The additional GHG emissions from alternative route n' due to MR&R activities performed on highway segment n are added to q_n instead of $q_{n'}$, and $q_{n'}(S_{n'}(t), x_{n'}(t))$ and $a_{n',j}(S_{n'}(t), x_{n'}(t))$ are independent of $x_n(t)$, $\forall n, \forall n' \neq n$.

To justify Assumption 1, the following discussion is necessary. While a roadway is under construction, no management activities are performed on the alternative routes because this may cause significant traffic capacity reduction. Therefore, unless most segments in a roadway network need maintenance actions urgently at the same time, it is reasonable to assume that GHG emissions from alternative routes, $q_{n'}(S_{n'}(t), x_{n'}(t))$, are not influenced by activities applied on a pavement segment, $x_n(t)$. Moreover, we do not account for possible cost savings from coordinated MR&R activities simultaneously performed on multiple adjacent segments.

Based on this discussion, Assumption 1 is realistic. Accordingly, $Q_{n'}(S_{n'}(0), x_{n'})$ and $A_{n',j}(S_{n'}(0), x_{n'})$ are independent of x_n , so we can derive Proposition 1.

Proposition 1. $Q_{n'}(S_{n'}(0), x_{n'}) + \sum_{j=1}^J \Lambda_j \cdot A_{n',j}(S_{n'}(0), x_{n'})$ is independent of x_n , $\forall n, \forall n' \neq n$.

The Lagrangian problem (3) is separable, based on Proposition 1, so the optimal policy under a certain set of Lagrangian multipliers, $x_{|\Lambda}$, is a set of segment-level policies, x_n for all segments, as expressed in (4).

$$x_{|\Lambda} = \left\{ \underset{x_n}{\operatorname{argmin}} Q_n(S_n(0), x_n) + \sum_{j=1}^J \Lambda_j \cdot A_{n,j}(S_n(0), x_n), \forall n \right\} \quad (4)$$

Based on the results obtained by solving (4), we can find the optimal Lagrangian multipliers by solving (5).

$$\mathcal{L}^*(S(0)) = \underset{\Lambda}{\operatorname{sup}} Q(S(0), x_{|\Lambda}) + \sum_{j=1}^J \Lambda_j \cdot [A_j(S(0), x_{|\Lambda}) - B_j] \quad (5)$$

The following two sub-sections, 3.1.1 and 3.1.2, will present the solution methodologies of the segment-level problem in (4) and the Lagrangian problem given in (5) respectively.

3.1.1 Dynamic programming algorithms for the segment-level problem

We address two different representations of the segment-level problem and their respective solution methodologies: (a) finite time horizon problem, where $T < \infty$; and (b) infinite time horizon problem, where $T \rightarrow \infty$. The complexities of both methodologies are polynomial in $|\mathbb{X}_n|$ and $|\mathbb{S}_n|$, which must be finite numbers to make the algorithms feasible. Because the number of pavement repair and maintenance options is limited in practice, $|\mathbb{X}_n|$ is finite. Regarding $|\mathbb{S}_n|$, we need to examine the possible ranges of roughness level and age:

- Severely deteriorated pavement surfaces associated with extensive area of fatigue cracking including alligator, longitudinal and reflection cracking in the wheel path (MEPDG Interim Guide 2008) cause significant traffic delays, vehicle wear and tear and user discomfort. Because the index of roughness reflects the area of fatigue cracking as well as length of transverse cracking and average rut depth, it is reasonable to introduce a maximum allowable roughness to prevent such problems. If roughness is equal to or higher than this level, either rehabilitation or reconstruction must be applied. Therefore, roughness has a range with a finite upper bound.

- Pavement structures with infinite age are unrealistic in practice, so all segments should be reconstructed in the infinite planning horizon problem. As for the finite horizon problem, age is finite by virtue of the fact that age cannot exceed the length of the planning horizon. Therefore, age is a finite number. Together with our previous observation that roughness is finite, we conclude that $|\mathbb{S}_n|$ is finite.

Finite horizon problem

Given finite T , the Dynamic programming for the segment-level problem (4) is presented by (6).

$$\mathcal{L}_n^T(S(T)|\Lambda) = 0$$

, and

$$\begin{aligned} \mathcal{L}_n^t(S(t)|\Lambda) = \min_{x_n(t)|\Lambda} E \left[\frac{1}{T-t} \left\{ q_n(S_n(t), x_n(t)) + \sum_{j=1}^J \Lambda_j \cdot a_{n,j}(S_n(t), x_n) \right\} \right. \\ \left. + \frac{T-t-1}{T-t} \mathcal{L}_n^{t+1}(S_n(t+1)|\Lambda) \right], \forall S_n(t) \in \mathbb{S}_n, t = 0, \dots, T-1 \end{aligned} \quad (6)$$

, where

$\mathcal{L}_n^T(S_n(T)|\Lambda)$: terminal Lagrangian function value at T for given $S_n(T)$ under Λ ;

$\mathcal{L}_n^t(S_n(t)|\Lambda)$: minimum expected average Lagrangian value from t until T , given state $S_n(t)$ under chosen Λ .

Program (6) is solved from $t = T$ to $t = 0$ recursively. There exists uncertainty regarding several parameters that influence GHG emissions in after the end of the planning horizon, so the terminal value is assumed to be zero.

Infinite horizon problem

An emission-free terminal state may seem unrealistic, which is why a steady state solution (Bertsekas, 2011) may be preferable. Such a solution can be obtained by solving an infinite horizon problem defined with $T \rightarrow \infty$. In the steady state, the segment-level policy, x_n , is a state-based policy that is independent of time. In other words, $x_n = \{x_n(S_n), \forall S_n \in \mathbb{S}_n\}$. The solution methodology for the infinite horizon

problem can be based on either Value Iteration or Policy Iteration, and is presented in detail in Appendix A.

3.1.2 Numerical algorithm for the Lagrangian problem

Once the segment-level policies have been determined, the problem becomes one of solving for the Lagrangian multipliers. The following numerical algorithm is proposed to find the optimal Lagrangian multipliers under an appropriate assumption such as the convexity of \mathcal{L} with respect to Λ .

Each iteration is indexed by k , and the Lagrangian multiplier vector in the iteration step is denoted by Λ^k . In step 1, we initialize the Lagrangian multipliers and the corresponding $x_{|\Lambda}$ obtained from (4). If $\Lambda = \mathbf{0}$, the Lagrangian problem is identical to the unconstrained problem addressed in (1) without the budget constraint (2a). If the unconstrained solution, x^0 , satisfies the budget constraints, it is not necessary to proceed to the next steps because the optimal solution is x^0 . If it does not, we update the Lagrangian multipliers in step 4, by using the gradient approximation method. Consequently, x^k is found based on the updated Λ^k in step 5. If $A_j(S(0), x^k) \leq B_j, \forall j$ and the solution converges, then x^k defines the optimal policy, and we terminate the iterations. If the solution converges but $\exists j, s. t. \Lambda_j = 0$, we terminate the algorithm because the problem is infeasible. Otherwise, we move to the next iteration.

Algorithm:

1. Set $k \leftarrow 0, \Lambda^0 \leftarrow 0$ and find $x^0 \leftarrow x_{|\Lambda^0}$.
2. If x^0 satisfies the budget constraints, then stop.
3. $k \leftarrow k + 1$,
4. Update Λ^k for all j by gradient approximation.
5. Find $x^k \leftarrow x_{|\Lambda^k}$.
6. If a termination condition is satisfied, then stop; otherwise, go to step 3.

3.2 Multiple budget expenditure period problem

If the problem is constrained by (2b) instead of (2a), the corresponding representations of the segment-level problem and Lagrangian problem are (7) and (8) respectively.

$$x_{|\Lambda} = \left\{ \underset{x_n}{\operatorname{argmin}} Q_n(S_n(0), x_n) + \sum_{w=1}^W \sum_{j=1}^J A_{j,w} \cdot A_{n,j,w}(S(T_0 + \dots T_{w-1}), x_n), \forall n \right\} \quad (7)$$

$$\mathcal{L}^*(S(0)) = \sup_{\Lambda} Q(S(0), x_{|\Lambda}) + \sum_{w=1}^W \sum_{j=1}^J A_{j,w} \cdot [A_{j,w}(S(T_0 + \dots T_{w-1}), x_{|\Lambda}) - B_j] \quad (8)$$

The solution for the finite horizon problem is:

$$\mathcal{L}_n^T(S(T)|\Lambda) = 0$$

, and

$$\begin{aligned} \mathcal{L}_n^t(S(t)|\Lambda) = \min_{x_n(t)|\Lambda} E \left[\frac{1}{T-t} \left\{ q_n(S_n(t), x_n(t)) + \frac{T}{T_w} \cdot \sum_{j=1}^J A_{j,w} \cdot a_{n,j}(S_n(t), x_n) \right\} \right. \\ \left. + \frac{T-t-1}{T-t} \mathcal{L}_n^{t+1}(S_n(t+1)|\Lambda) \right] \quad (9) \end{aligned}$$

, if $(T_0 + \dots T_{w-1}) \leq t \leq (T_0 + \dots T_w) - 1, \forall S_n(t) \in \mathbb{S}_n$.

The solution for the infinite horizon problem, where $T_w < \infty$ and $W \rightarrow \infty$, is the same as shown in Section 3.1.1 because it is in the steady state.

For the Lagrangian problem, the numerical method presented in Section 3.1.2 can be used.

4. Case Study

A highway system consisting of 311 AC pavement segments, selected from Caltrans District 4 in California, is used to test our optimization model. For every segment, information regarding traffic volume, traffic loading, structural design and lane number is available.

The deterioration process of the surface layer is stochastic. We use Paterson's pavement roughness progression model, which accounts for the effects of age, average daily traffic loading and pavement design (Paterson, 1987). This prediction model has a mathematical closed form and provides the standard deviations of all model coefficients. Therefore, by combining the improvement models

(the effect of the maintenance and rehabilitation activities) with the deterioration model, we can obtain probabilistic prediction of the deterioration process.

The data set at our disposal does not specify the IRI and ages of the pavements. Thus, we randomly generate the current roughness levels and ages for the pavement segments to be uniformly distributed between 1.2 m/km and 2.0 m/km (i.e. $s_n(0) \leftarrow Unif(1.2, 2)$) and 0 and 20 years, (i.e. $h_n(0) \leftarrow Unif(0, 20)$) respectively.

The cost and emission models might vary in the future due to rapid advances in vehicle technology. Further, future budget allocations remain unpredictable. For these reasons, we solve the finite planning horizon problem over a 40-year time period rather than the infinite planning horizon problem. The unit time period is 3 months, i.e. $T = 160$, and the maximum allowable roughness is 6 IRI. However, in this section, we use year as a unit of time instead of 3 months to present numbers for convenience, e.g. MT CO₂e/year instead of MT CO₂e/3-months. We assume flexibility of budget allocation between periods along the planning horizon, i.e. the problem is constrained by (2a).

In terms of budget scenarios, we consider two cases:

- (a) all activities are funded from a single combined budget, $J = 1$; and
- (b) activities are funded from two separate budget sources, $J = 2$.

In the first scenario, reconstruction, rehabilitation, and maintenance activities are funded from a combined single budget, whereas in the second, reconstruction projects are financed by a capital budget $j = 1$, but maintenance and rehabilitation activities are financed by a maintenance budget $j = 2$. Reconstruction and rehabilitation cannot be carried out together in the same period, and the timing of the treatments is assumed to be at the starting point of the period. Reconstruction and rehabilitation improve condition state instantly, but maintenance activities, such as bituminous surface treatments, non-structural overlay, crack sealing, slurry sealing, fog sealing, etc., are performed frequently and almost continuously over a period.

In short, \mathbb{x}_n , consists of six options: (a) do-nothing during the period; (b) rehabilitation only at the starting point of the period; (c) reconstruction only at the starting point of the period; (d)

maintenance only over the period,.; (e) rehabilitation at the starting point of the period and maintenance over the period; and (f) reconstruction at the starting point of the period and maintenance over the period.

The emission and cost models for users and the interventions are presented in Appendix B. GHG emissions due to routine maintenance activities are insignificant (and assumed to be zero) compared to the emissions produced from the other activities. For instance, for crack sealing, one of the routine maintenance activities, the total amount of material is much lower than that of major rehabilitation and reconstruction activities (Smith and Romine, 2001). Moreover, because of its duration and number of closed lanes, the traffic disruptions can be considered negligible.

4.1 Case study results

Figure 1 illustrates how the objective emissions changes with respect to the combined agency budget. The agency budget at the left end of the curve is the total agency cost necessary to maintain the network with minimal interventions while satisfying the worst-case constraints of maximum allowable roughness and maximum lifecycle length. If the available budget is lower than the lower bound, it is impossible to keep the network above the minimum standards.

The right-end point represents the agency budget necessary to minimize the total GHG emissions. At this point, $\lambda_1 = 0$. To the right of this point, the budget constraint is not binding, and the optimal objective value and policy are same as those at this point. The curve can be interpreted as a Pareto frontier obtained from the bi-objective optimization problem minimizing emissions and agency costs. The Pareto frontier shows that significant reductions in GHG emissions can be achieved with small increases in budget, if the current budget is small, and that there are decreasing marginal improvements in GHG emissions reduction. Figure 1 also shows that for this system of pavements, a total reduction in GHG emissions of 20% from 23,460 MT CO₂e/year to 18,930 MT CO₂e/year is possible if the total budget is increased by 35% from \$ 3.71 M/year to \$5.50 M/year.

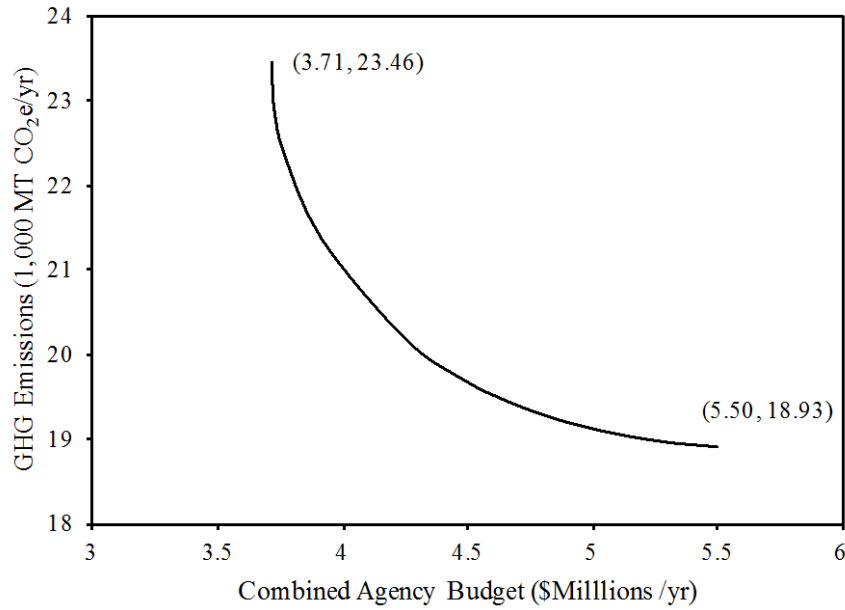


Figure 1. Possible minimum annual GHG emissions from highway users and MR&R activities, Q^* , as a function of combined annual agency budget, B_1 ($J = 1$)

The optimal proportions of reconstruction, rehabilitation and maintenance projects in the combined agency budget are shown in Figure 2. As seen in this figure, as the budget increases, the importance of rehabilitation and maintenance activities increases to reduce total users' emissions by keeping pavements in good condition. The proportion of capital costs allocated to reconstruction, relative to rehabilitation, decreases as the budget increases. This is because the combination of more intensive maintenance and rehabilitations makes reconstruction less necessary.

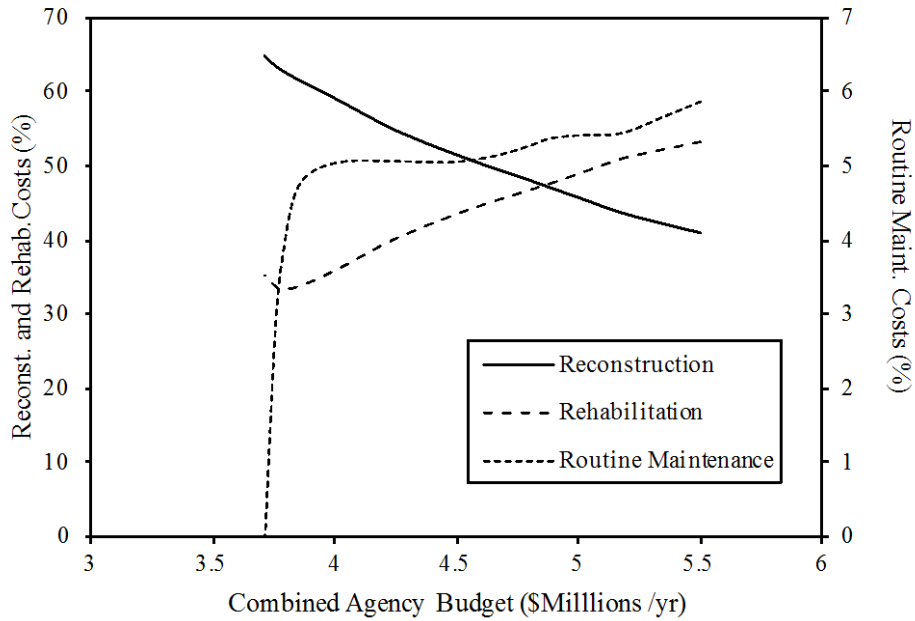


Figure 2. Optimal budget proportions of MR&R activities (%) under a combined annual budget, B_1 ($J = 1$)

Figure 3 represents optimal policy regimes in the case of separate budgets. The x-axis refers to the capital budget, B_1 , the y-axis stands for the maintenance budget, B_2 , and the optimal emissions for given budget situations, $Q_{|B_1, B_2}^*$, are represented by different gray shades according to their values. Point (a) is located at the optimum in the unconstrained problem, i.e. minimization of GHG emissions without budget constraints. If a budget situation is located in region A, it has the same optimal solution as that of point (a), and both constraints are not binding.

Point (b) represents the optimal maintenance budget when the capital budget is zero. The case study has a finite planning horizon, so it is possible to have no reconstruction in the planning horizon, which is why point (b) is located on the y-axis. If the capital budget is zero, the highest maintenance budget is necessary to satisfy the other constraints at optimality. In region B, the area above the line between (a) and (b), the capital budget is binding and the maintenance budget is not binding at optimality. The line between (a) and (b) is equivalent to the optimal solutions found for the GHG emissions minimization problem constrained only by the capital budget.

Point (c) shows the optimal capital budget for a zero maintenance budget. In this situation, only reconstructions are performed on all of the segments during the planning horizon. Region C is defined as the right side of the line between points (a) and (c), and a situation in C has a binding maintenance budget constraint and a non-binding capital constraint.

Line \overline{ad} is identical to the optimal solution found for the combined budget problem, $J = 1$. In other words, Λ_1 is equal to Λ_2 on \overline{ad} . Point (a) corresponds to the right-end point in Figure 1, and point (d) matches the left-end point. As shown in Figure 2, rehabilitation and routine maintenance costs increase while reconstruction costs decrease as a combined budget increases (from point (d) to point (a)).

Line \overline{edc} represents the boundary between the feasible region and the infeasible region. In the infeasible region F, there is no policy to satisfy the maximum allowable roughness constraint. The area between \overline{edc} and \overline{bac} can be divided into two regions, D and E, separated by \overline{ad} . In both regions, both budget constraints are binding. In region D, Λ_1 is bigger than Λ_2 , while Λ_2 is bigger than Λ_1 in region E.

In regions D and E, the 3-dimensional solution plane $(Q_{|B_1, B_2}^*, B_1, B_2)$ is interpreted as a Pareto frontier obtained from the multi-criteria problem considering: i) GHG emission; ii) capital costs; and iii) maintenance costs. The Pareto frontier is useful as it allows decision makers to focus on tradeoffs among the expected GHG emissions and multiple budgets only within range of optimal policies, contained entirely in regions D and E.

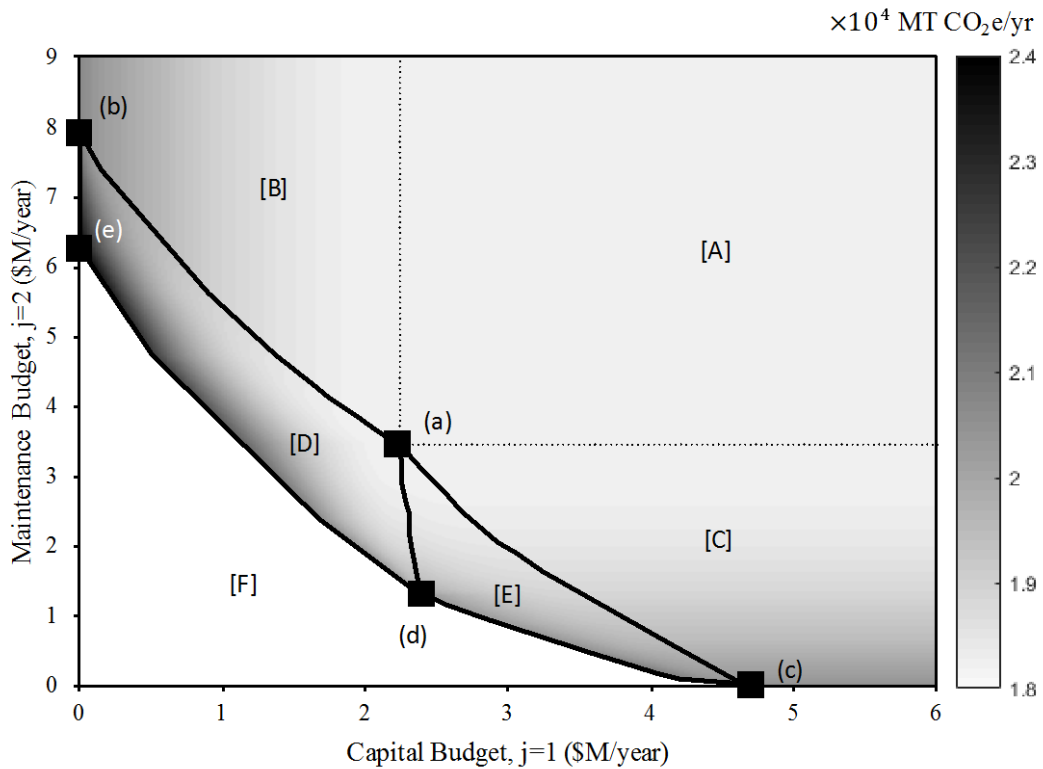


Figure 3. Possible minimum annual GHG emissions from highway users and MR&R activities, Q^* , with two-dimensional budget situations: capital budget, B_1 , on the x-axis; and maintenance budget, B_2 , on the y-axis

4.2 Sensitivity analysis results

The magnitude of traffic delays is one of the largest sources of uncertainty in our analysis is because they depend on the network topology, which is not accounted for in our model, and driver behavior, which is difficult to predict. The sensitivity of the results with respect to traffic delays due to highway closures during rehabilitation and construction is examined. As for the other sources of uncertainty, Reger et al. (2015) showed that the solutions considering rehabilitation only are robust with respect to the pavement deterioration rate and percentage change in fuel consumption. The GHG emissions from a reconstruction project are mainly affected by roadway closure and materials. The sensitivity with respect to the former is examined here. We assume that the amount of materials and corresponding emissions are relatively deterministic compared to the other variables.

Figure 4 shows the effect of different traffic delays from reconstruction and rehabilitation activities, for two cases: a 20% reduction and a 20% increase from the original level under a combined budget ($J = 1$) reflecting situations where traffic delays are overestimated and underestimated respectively. There is almost no difference (about 2%) in the emission levels among scenarios if the budget is \$ 3.8 M/year. This is because the possible number of rehabilitations and reconstructions throughout the planning horizon is limited due to the low budget, so the fluctuation of traffic delays during these interventions does not bring a significant effect on the total emissions. However, if the budget is sufficient to perform frequent rehabilitations and reconstructions, the impacts of the traffic delay variations on both the optimal emission and the optimal management policy increase. We can conclude that the optimal solution is robust to traffic delays changes under low budgets but more sensitive for high budgets. Therefore, as expected intuitively, it is more important to analyze the traffic impacts of interventions accurately when available budgets are high.

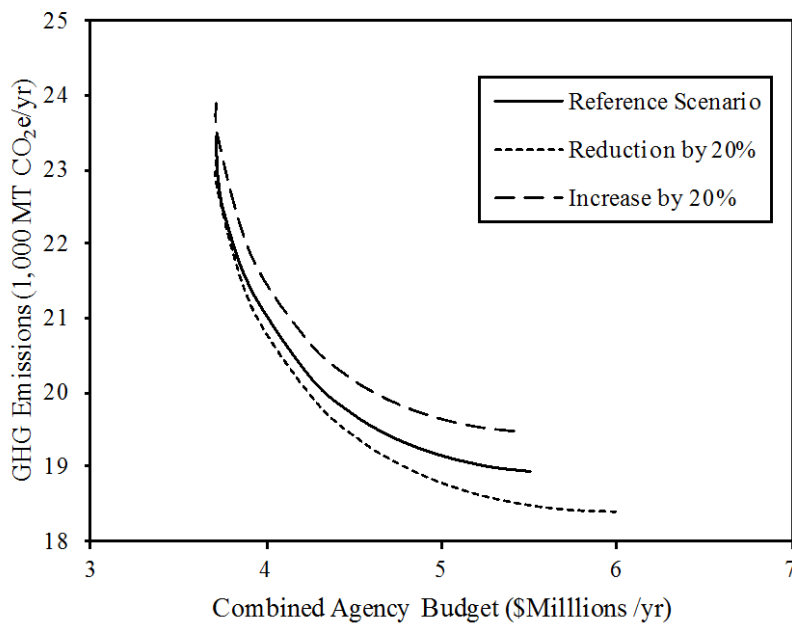


Figure 4 Sensitivity Analysis of the possible minimum annual GHG emissions from highway users and MR&R activities, Q^* , to traffic delays due to highway closures, $B_1 = \$ 3.71$ M/year ($J = 1$)

5. Conclusion

In this paper, we addressed the optimization problem of minimizing GHG emissions under single or multiple budget constraints. The bottom-up solution algorithm uses Lagrangian Relaxation and Dynamic Programming.

A case study is presented using a system of pavement segments in California. The results indicate the possibility of reduction in GHG emissions by 20% through increasing the total budget by 35% on the Pareto frontier. For the case of different budget sources for maintenance and reconstruction, we obtain a Pareto frontier that provides the minimum emissions achievable subject to different budget constraints.

The sensitivity analysis results show that the solution is robust with respect to the uncertainty in forecasting traffic delays when agency budgets are low. As the available budget increases, the optimal results become more sensitive to uncertainty.

The main limitation of our work is that we do not account for functional or economic interdependence among pavement segments in networks. For example, because consecutive segments comprise a network link, a partial or complete closure of a segment yields a capacity drop through the link. Therefore, cost savings can be achieved by clustering rehabilitation or construction activities on segments in the same year, even if the optimal timings of these activities are different across segments. Likewise, reconstruction of a segment on a link may lead to traffic diversion to an alternate route, thus increasing GHG emissions on it. Accounting for network interdependencies such as these adds significant complexities that are beyond the scope of this paper. It may be possible to account for these interdependencies by using tools such as Approximate Dynamic Programming, which have been used to address them (Medury and Madanat, 2013).

Acknowledgement

Funding for this research was provided by the NYUAD research funds of the second author. We are grateful to John Harvey who provided us with the data for the case study. We also appreciate the valuable comments of the anonymous reviewers.

Appendix A Steady State Solution Algorithm

The steady state solution methodology is presented in this Appendix. Since $T = \infty$, the problem (4) is a general average problem, where the optimal average values are independent of the initial state (Lee et al. 2016). Therefore, the initial state $S(0)$ is omitted from the representation of the function and the inner problem is expressed as (A.1), where $H_{n|\Lambda}^*$ is the optimal value of $Q_n(x_n) + \sum_{j=1}^J \Lambda_j \cdot A_{n,j}(x_n)$.

$$H_{n|\Lambda}^* = \min_{x_n} Q_n(x_n) + \sum_{j=1}^J \Lambda_j \cdot A_{n,j}(x_n), \forall \quad (\text{A.1})$$

The problem (A.1) has a same optimal policy, x_n^* , as a shortest path problem with the stage value presented in (A.2) (Bertsekas, 1998). This stage value is the difference between the original stage value, which is the expected term expressed in (A.2), and its average value along the infinite time horizon, $H_{n|\Lambda}^*$.

$$E \left[q_n(S_n, x_n(S_n)) + \sum_{j=1}^J \Lambda_j \cdot a_{n,j}(S_n, x_n(S_n)) \right] - H_{n|\Lambda}^* \quad (\text{A.2})$$

The optimal objective value of the shortest path problem is denoted by $h_n^*(S_n|\Lambda)$, and its Bellman Equations is:

$$h_n^*(S_n|\Lambda) = \min_{x_n(S_n) \in \mathbb{X}_n} E \left[q_n(S_n, x_n(S_n)) + \sum_{j=1}^J \Lambda_j \cdot a_{n,j}(S_n, x_n(S_n)) + E[h_n^*(S'_n|\Lambda)] \right] \quad (\text{A.3})$$

$$-H_{n|\Lambda}^*, \forall S_n \in \mathbb{S}_n,$$

, where

S'_n : pavement state at the end of the period associated with the transition probability, $f(S'_n|S_n, x_n(S_n))$.

The above Bellman equation is solved by either of two iteration methods, commonly known as the value iteration and the policy iteration. In this paper, we briefly present the relative value iteration algorithm, which is equivalent to the value iteration method, and the policy iteration algorithm. In the algorithms, S_{new} refers to the best state, typically achievable by reconstruction; it is known to be a recurrent state as shown in Lee et al. (2016). A mathematical proof of this result can be found in Bertekas (1998).

Algorithm A1. Relative Value Iteration:

1. Set iteration index $k \leftarrow 0$, and initialize $h_n^0(S_n|\Lambda)$ for all $S_n \in \mathbb{S}_n$.
2. $k \leftarrow k + 1$
3. Update $h_n^k(S_n|\Lambda)$ for all $S_n \in \mathbb{S}_n$ by (A.4).
4. If $h_n^k(S_n|\Lambda) = h_n^{k-1}(S_n|\Lambda)$, the algorithm terminates; otherwise, go to step 1.

$$\begin{aligned}
 h_n^k(S_n|\Lambda) &= \min_{x_n(S_n) \in \mathbb{X}_n} \left[E \left[q_n(S_n, x_n(S_n)) + \sum_{j=1}^J \Lambda_j \cdot a_{n,j}(S_n, x_n(S_n)) + h_n^{k-1}(S'_n|\Lambda) \right] \right] \\
 &- \min_{x_n(S_{new}) \in \mathbb{X}_n} \left[E \left[q_n(S_n, x_n(S_{new})) + \sum_{j=1}^J \Lambda_j \cdot a_{n,j}(S_n, x_n(S_{new})) + h_n^{k-1}(S'_{new}|\Lambda) \right] \right]
 \end{aligned} \tag{A.4}$$

Algorithm A2. Policy Iteration:

1. Set iteration index $k \leftarrow 0$, and initialize $x_n^0(S_n)$ and $h_n^0(S_n|\Lambda)$ for all $S_n \in \mathbb{S}_n$.
2. $k \leftarrow k + 1$.
3. Calculate $H_{n|\Lambda}^k$ and $h_n^k(S_n|\Lambda)$ by (A.5).
4. Update $x_n^k(S_n)$ for all $S_n \in \mathbb{S}_n$ by (A.6).
5. If $H_{n|\Lambda}^k = H_{n|\Lambda}^{k-1}$ and $h_n^k(S_n|\Lambda) = h_n^{k-1}(S_n|\Lambda)$, the algorithm terminates; otherwise, go to step 1.

$$h_n^k(S_{new}|\Lambda) = 0$$

, and

$$h_n^k(S_n|\Lambda) + H_{n|\Lambda}^k = E \left[q_n(S_n, x_n^{k-1}(S_n)) + \sum_{j=1}^J \Lambda_j \cdot a_{n,j}(S_n, x_n^{k-1}(S_n)) + h_n^k(S'_n|\Lambda) \right] \tag{A.5}$$

$$x_n^k(S_n) = \underset{x_n(S_n) \in \mathbb{X}_n}{\operatorname{argmin}} E \left[q_n(S_n, x_n(S_n)) + \sum_{j=1}^J \Lambda_j \cdot a_{n,j}(S_n, x_n(S_n)) + h_n^k(S'_n|\Lambda) \right], \forall S_n \tag{A.6}$$

Appendix B Emission, Cost and Performance Models

Pavement deterioration and improvement models are presented in (B.1), where τ is a unit period length and l_n refers to the annual average traffic loading. The AC pavement structures have three layers including hot mix asphalt (HMA), $i = 1$, aggregate sub-base, $i = 2$, and aggregate base, $i = 3$, and their thickness are denoted by ρ^i . The coefficients are: $\beta^1=0.0173/\text{mm}$; $\beta^2=0.00551/\text{mm}$; and $\beta^3=0.00433/\text{mm}$ (AASHTO, 1933). The random parameters are: $\alpha \sim TN(725, 94400, 0, \infty)$; $b \sim TN(0.08, 7.3 \times 10^7, 0, \infty)^*$; $q \sim TN(-4.99, 0.064, -\infty, 0)$. Here, TN stands for the truncated normal distribution.

$$S_n(t+u) = \{s_n(t+u), h_n(t+u)\} \\ = \left\{ s_n(t)e^{bu} + \alpha \cdot u \cdot \left(\sum_{i=1,2,3} [\beta^i \cdot \rho^i] + 1 \right)^q \cdot l_n \cdot e^{b(h_n(t)+u)}, h_n(t) + u \right\}, \forall u \in (0, \tau) \quad (\text{B.1})$$

The user emission model due to lower fuel efficiency from higher roughness on segment n is represented in (B.2), where $AADT_n$ is the annual average traffic volume and $AADTT_n$ is the annual average truck traffic volume. The coefficients are $e_1 = 0.0028917 \text{ kg-CO}_2\text{e/IRI-km-car}$ and $e_2 = 0.0075516 \text{ kg-CO}_2\text{e/IRI-km-truck}$ (Horvath, 2004).

$$\int_0^\tau (e_1 \cdot (AADT_n - AADTT_n) + e_2 \cdot AADTT_n) \cdot s_n(t+u) du \quad (\text{B.2})$$

The costs and performance models of routine maintenance are expressed in (B.3) and (B.4) respectively, where D_n is the lane number of segment n . The cost parameters are: $c_1 = 88\$/\text{lane-km-year}$; $c_2 = 120$; and $c_3 = 440\$/\text{lane-km-year}$ (Gu et al. 2012).

$$\tau \cdot D_n \cdot (c_1 e^{c_2 \Delta b} + c_3) \quad (\text{B.3})$$

$$S_n(t+u) = \\ \left\{ s_n(t)e^{(b-\Delta b)u} + a \cdot u \cdot \left(\sum_{i=1,2,3} [\beta^i \cdot \rho^i] + 1 \right)^q \cdot l_n \cdot e^{(b-\Delta b)(h_n(t)+u)}, h_n(t) + u \right\}, \forall u \in (0, \tau] \quad (\text{B.4})$$

The costs, performance and emission models of rehabilitation are expressed in (B.5), (B.6) and (B.7) respectively (Lee and Madanat 2015a), where s_0 refers to the best achievable roughness by rehabilitation, and t^+ stands for the time point following the time point t when the rehabilitation is

performed. The coefficients are: $\mu_1 = 0.66$; $\mu_2 = 7.15$ mm/IRI; $\mu_3 = 18.3$ mm (Ouyang and Madanat 2004); $m_1 = 413$ \$/lane-km-mm; $m_2 = 33,012$ \$/lane-km; and $e_3 = 225$ kg-CO₂e/lane-km-mm (Horvath, 2004).

$$D_n \cdot \frac{\mu_2 + \frac{\mu_3}{s_n(t)}}{\mu_1} \cdot \max[0, \min[s_n(t) - s_0, \mu_1 \cdot s_n(t)]] \cdot m_1 + D_n \cdot m_2 \quad (\text{B.5})$$

$$s_n(t^+) = \{\min(s_n, \max(s_0, (1 - \mu_1) \cdot s_n)), h_n\} \quad (\text{B.6})$$

$$D_n \cdot \max[0, \min[s_n(t) - s_0, \mu_1 \cdot s_n(t)]] \cdot e_3 \quad (\text{B.7})$$

The reconstruction cost, performance and emission models are shown in (B.8), (B.9) and (B.10) respectively. The coefficients are: $m_3^1 = 125.2$ \$/lane-km-mm, $m_3^2 = 39.8$ \$/lane-km-in, and $m_3^3 = 31.3$ \$/lane-km-in. $m_4 = 57,380$ \$/lane-km, $e_4^1 = 539.3$ kg-CO₂e/lane-km-mm and $e_4^2 = e_4^3 = 136.8$ kg-CO₂e/lane-km-mm (Horvath, 2004). The user emissions resulting from the traffic disruption are approximately 20% of the total emissions from the construction, so scaling factor γ_n is multiplied.

$$\sum_{i=1,2,3} [D_n \cdot \rho^i \cdot m_3^i] + D_n \cdot m_4 \quad (\text{B.8})$$

$$s_n(t^+) = \{s_{new}, 0\} \quad (\text{B.9})$$

$$\gamma_n \cdot \sum_{i=1,2,3} D_n \cdot \rho^i \cdot e_4^i \quad (\text{B.10})$$

References

- American Association of State Highway and Transportation Officials (AASHTO), 1993. AASHTO Guide for Design of Pavement Structures, 1. AASHTO.
- Bellman, R., 1956. Dynamic programming and Lagrange multipliers. *Proceedings of the National Academy of Sciences*, 42 (10), pp.767-769.
- Bertsekas, D., 1998. A new value iteration method for the average cost dynamic programming problem. *SIAM Journal on Control and Optimization*, 36, pp. 742-759.
- Bertsekas, D., 2011. *Dynamic Programming and Optimal Control 3rd Edition*. Belmont, MA: Athena Scientific.
- California Department of Transportation (Caltrans), 2015. *State of the pavement, 2015*. State of California Department of Transportation, Division of Maintenance, Sacramento, CA.
- Environmental Protection Agency (EPA), 2017. *Inventory of US greenhouse gas emissions and sinks: 1990-2015*.
- Forster, P., Ramaswamy, V., Artaxo, P., Berntsen, T., Betts, R., Fahey, D., Haywood, J., Lean, J., Lowe, D., Myhre, G., Nganga, J., 2007. Changes in atmospheric constituents and in radiative forcing. Chapter 2. In *Climate Change 2007. The Physical Science Basis*.
- Gosse, C., Clarens, A., 2013. Quantifying the total cost of infrastructure to enable environmentally preferable decisions: the case of urban roadway design. *Environmental Research Letters*, 8 (1), p. 015028.
- Gu, W., Ouyang, Y., Madanat, S., 2012. Joint optimization of pavement maintenance and resurfacing planning. *Transportation Research Part B*, 46 (4), pp. 511–519.
- Horvath, A., 2004. *Pavement Life-cycle Assessment Tool for Environmental and Economic Effects (PaLATE)*. Available from: <<http://ce.berkeley.edu/~horvath/palate.html>> (accessed 24 March, 2014)
- Kendall, A., 2012. Time-adjusted global warming potentials for LCA and carbon footprints. *The International Journal of Life Cycle Assessment*, 17 (8), pp.1042-1049.

- Lee, J., Madanat, S., 2014. Joint optimization of pavement design, resurfacing and maintenance strategies with history-dependent deterioration models. *Transportation research part B*, 68, pp. 141-153.
- Lee, J., Madanat, S., 2015a. Jointly optimal policies for pavement maintenance, resurfacing and reconstruction. *EURO Journal on Transportation and Logistics*, 4 (1), pp. 75-95.
- Lee, J., Madanat, S., 2015b. A joint bottom-up solution methodology for system-level pavement rehabilitation and reconstruction. *Transportation Research Part B*, 78, pp. 106-122.
- Lee, J., Madanat, S., Reger, D., 2016. Pavement systems reconstruction and resurfacing policies for minimization of life-cycle costs under greenhouse gas emissions constraints. *Transportation Research Part B*, 93, pp. 618-630.
- Lidicker, J., Sathaye, N., Madanat, S., Horvath, A., 2012. Pavement resurfacing policy for minimization of life-cycle costs and greenhouse gas emissions. *Journal of Infrastructure Systems*, 19 (2), pp. 129-137.
- Medury, A., Madanat, S., 2013. Incorporating network considerations into pavement management systems: A case for approximate dynamic programming. *Transportation Research Part C*, 33, pp. 134-150.
- MEPDG (Mechanistic-Empirical Pavement Design Guide) Interim Guide, 2008. Mechanistic-empirical pavement design guide: A manual of practice, AASHTO, Washington, DC.
- Ouyang, Y., Madanat, S., 2004. Optimal scheduling of rehabilitation activities for multiple pavement facilities: exact and approximate solutions. *Transportation Research Part A*, 38 (5), pp. 347-365.
- Paterson, W., 1987. *Road Deterioration and Maintenance Effects: Models for Planning and Management*. Johns Hopkins University Press, Baltimore, MD.
- Rashid, M., Tsunokawa, K., 2012. Trend curve optimal control model for optimizing pavement maintenance strategies consisting of various treatments. *Computer-Aided Civil and Infrastructure Engineering*, 27 (3), pp. 155-169.
- Reger, D., Madanat, S., Horvath, A., 2014. Economically and environmentally informed policy for road resurfacing: tradeoffs between costs and greenhouse gas emissions. *Environmental Research Letters*, 9, p. 104020

- Reger, D., Madanat, S., Horvath, A., 2015. The effect of agency budgets on minimizing greenhouse gas emissions from road rehabilitation policies. *Environmental Research Letters*, 10 (11), p. 114007.
- Santero, N., Masanet, E., Horvath, A., 2011. Life-cycle assessment of pavements. Part I: Critical review. *Resources, Conservation and Recycling*, 55 (9), pp. 801-809.
- Sedjo, R., Marland, G., 2003. Inter-trading permanent emissions credits and rented temporary carbon emissions offsets: some issues and alternatives. *Climate Policy*, 3 (4), pp. 435-444.
- Smith, K., Romine, A., 2001. *Materials and Procedures for Sealing and Filling Cracks in Asphalt-surfaced Pavements--manual of Practice* (No. FHWA-RD-99-147,).
- Wang, T., Harvey, J., Kendall, A., 2014. Reducing greenhouse gas emissions through strategic management of highway pavement roughness. *Environmental Research Letters*, 9 (3), p. 034007.
- Wang, T., Lee, I., Kendall, A., Harvey, J., Lee, E., Kim, C., 2012. Life cycle energy consumption and GHG emission from pavement rehabilitation with different rolling resistance. *Journal of Cleaner Production*, 33, pp. 86-96.
- Watanatada, T., Dhareshwar, A., Lima, P., 1987. *Vehicle speeds and operating costs: Models for road planning and management*, The Johns Hopkins University Press, Baltimore, MD.
- Zaabar, I., Chatti, K., 2010. Calibration of HDM-4 models for estimating the effect of pavement roughness on fuel consumption for US conditions. *Transportation Research Record*, 2155, pp. 105-116.